Exp Brain Res (2012) 219:1–11
DOI 10.1007/s00221-012-3059-y

RESEARCH ARTICLE

Neural correlates of oddball detection in self-motion heading: A high-density event-related potential study of vestibular integration

H. Nolan · J. S. Butler · R. Whelan · J. J. Foxe · H. H. Bülthoff · R. B. Reilly

Received: 9 September 2011 / Accepted: 2 March 2012 / Published online: 21 March 2012

Abstract The perception of self-motion is a product of the integration of information from both visual and non-visual cues, to which the vestibular system is a central contributor. It is well documented that vestibular dysfunction leads to impaired movement and balance, dizziness and falls, and yet our knowledge of the neuronal processing of vestibular signals remains relatively sparse. In this study, high-density electroencephalographic recordings were deployed to investigate the neural processes associated with vestibular detection of changes in heading. To this end, a self-motion oddball paradigm was designed. Participants were translated linearly 7.8 cm on a motion platform using a one second motion profile, at a 45° angle leftward or rightward of straight ahead. These headings were presented with a stimulus probability of 80–20 %. Participants responded when they detected the infrequent direction change via button-press. Event-related potentials (ERPs) were calculated in response to the standard (80 %) and target (20 %) movement directions. Statistical parametric mapping showed that ERPs to standard and target movements differed significantly from 490 to 950 ms post-stimulus. Topographic analysis showed that this difference had a typical P3 topography. Individual participant bootstrap analysis revealed that 93.3 % of participants exhibited a clear P3 component. These results indicate that a perceived change in vestibular heading can readily elicit a P3 response, wholly similar to that evoked by oddball stimuli presented in other sensory modalities. This vestibular-evoked P3 response may provide a readily and robustly detectable objective measure for the evaluation of vestibular integrity in various disease models.

Keywords Electroencephalography · Evoked potentials · Vestibular · Heading · Self-motion · P3 · Cognition

H. Nolan and J. S. Butler contributed equally to the paper.

Electronic supplementary material The online version of this article (doi:10.1007/s00221-012-3059-y) contains supplementary material, which is available to authorized users.

H. Nolan · R. Whelan · R. B. Reilly
The Trinity Centre for Bioengineering,
Trinity College Dublin, Dublin, Ireland
e-mail: richard.reilly@tcd.ie

J. S. Butler · H. H. Bülthoff
Max Planck Institute for Biological Cybernetics,
Tübingen, Germany

J. S. Butler (✉) · J. J. Foxe
The Sheryl and Daniel R. Tishman Cognitive Neurophysiology Laboratory, Children's Evaluation and Rehabilitation Center (CERC), Departments of Pediatrics and Neuroscience,
Albert Einstein College of Medicine, Bronx, NY, USA
e-mail: john.butler@einstein.yu.edu

R. Whelan
Department of Psychology, University of Vermont,
Burlington, VT, USA

H. H. Bülthoff
Department of Brain and Cognitive Engineering,
Korea University, Seoul, South Korea

Introduction

The perception of self-motion is driven by inputs from a combination of different sensory modalities, the most obvious of which are visual, vestibular, and proprioceptive signals. The vestibular system, the focus of the current study, detects both linear and rotational motion, even when individuals have no visual inputs to rely upon (see Lopez and Blanke 2011; Angelaki and Cullen 2008). Recent

advances in experimental methodologies have made it possible to perform electrophysiological recordings in non-human primates while they are passively translated and/or rotated, providing insight into the neuronal processing of vestibular signals (Bremmer et al. 2002a, b; Gu et al. 2007, 2008, 2010; Fetsch et al. 2010). Specifically, Gu and colleagues (2007, 2008) showed a functional link between medial superior temporal (MST) activity and behavioral heading discrimination for purely vestibular signals, which suggests that vestibular cues can be processed in a unisensory manner as well as in a multisensory manner, akin to other sensory modalities. In accord with these results in animal models, recent human behavioral studies have shown that vestibular-alone cues can be used to accurately discriminate heading (Telford et al. 1995; Ohmi 1996; Fetsch et al. 2009; Butler et al. 2010; de Winkel et al. 2010; MacNeilage et al. 2010), although some evidence also points to interference effects from entirely veridical vestibular inputs under certain multisensory stimulation conditions (Telford et al. 1995; de Winkel et al. 2010; Butler et al. 2011).

To date, only a few studies have investigated electrophysiological responses to self-motion perception in humans. These have mainly been event-related potential (ERP) studies that aimed to detail the primary sensory responses of the vestibular system to short rotational stimuli (Hood and Kayan 1985; Kolchev 1995; Rodionov et al. 1996; Loose et al. 2002). While these measures have shown some potential for clinical research applications (Hofferberth 1995), the step profiles involved are not particularly representative of motion in an everyday context, and problems such as electrooculogram (EOG) and electromyogram (EMG) artifacts from rotational stimuli are frequently reported. That is, EOG artifacts are essentially unavoidable during rotational motion due to the vestibulo-ocular reflex (see e.g., Hofferberth 1995; Kolchev 1995; Rodionov et al. 1996). Thus, the clinical utility of these measures remains somewhat limited.

Our previous work and others show, however, that these problems are avoidable during linear self-motion conditions (Nolan et al. 2009, 2011a, b, Gramann et al. 2010; Gwin et al. 2010). By translating individuals using a so-called "Stewart Platform" to generate linear motion trajectories, high-quality EEG signals can be recorded without noticeable electromagnetic, EOG or EMG interference (Nolan et al. 2009, 2011a, b). Building upon these results, here we investigate change detection of vestibular heading while recording high-density event-related potentials (ERPs) from 128 scalp channels. For our purposes here, we adapted the classical two-stimulus oddball paradigm (Polich 1993) whereby participants are presented a stream of frequent standard stimuli (80 %) that is interrupted by occasional target stimuli (20 %), with the requirement that they respond when they detect a target stimulus—in this case, a change in the direction of heading. It has been shown using similar infrequent changes in visual, auditory, somatosensory, and olfactory inputs that the target stimulus elicits the now classic P3 component of the ERP when the novel deviant is detected (Sutton et al. 1965; Morgan et al. 1999). This response has been extensively studied and it is clear that it is associated with evaluative cognitive processes for detected novel events (e.g., Friedman et al. 2001). Two distinct subcomponents have been identified, a frontal P3a that is associated with stimulus-driven attentional orienting and a more posterior tempero-parietal P3b that has been associated with memory processing (e.g., Polich 2007). Because this P3 complex is such a robust and easily recorded ERP metric, it has excellent properties for use as an index of integrity of vestibular function. Here, we sought to induce vestibular-evoked P3 responses, with an eye to establishing this technique as an easily deployable measure of vestibular integrity and the perception of self-motion.

Methods

Participants

Sixteen neurologically typical participants with normal or corrected-to-normal vision, per self-report, participated in this experiment. The age range was 22–35 (mean 28.1 ± SD 3.9). Participants gave their written consent before taking part in the experiment, which was performed in accordance with the ethical standards laid down in the 1964 Declaration of Helsinki. One participant was subsequently removed from the study due to excessively noisy data.

Apparatus

A Maxcue 600 platform manufactured by Motion-Base PLC (von der Heyde 2001) was employed. This is a 6-legged Stewart platform with 6 degrees of freedom, which are rotation and translation about 3 axes (see Fig. 1a, b). A fixation cross was displayed on a projection screen, with a field of view of 86° × 65°, a resolution of 1,400 × 1,050 and a refresh rate of 60 frames per second. Participants wore Sennheiser HD600 headphones with one-way communication capability while white noise was played to mask the sound of the platform motors. Participants responded only to target stimuli using a single button on a four button response box. EEG data were recorded using a Biosemi ActiveTwo^{TM} 128 channel EEG (http://www.biosemi.com) system with 7 supplementary electrodes recording EOG and EMG. The data acquired with the Biosemi were sampled at 512 Hz. Data were referenced offline to the common average reference.

Vestibular oddball heading paradigm

The classical oddball paradigm, in which an infrequent target is identified in a sequence of frequent standard stimuli (Katayama and Polich 1999), was adapted for heading stimuli.

The one second motion displacement profile, s(t), had a sigmoid shape and was described by:

$$s(t) = 0.49\frac{(2\pi t - \sin(2\pi t))}{4\pi^2} \quad 0 < t \leq 1s$$

where t is time in seconds and 2π is the angular frequency of the sinusoid acceleration profile. The maximum displacement, velocity, and acceleration were 0.078 m, 0.156 m/s, and 0.49 $m/s^{2,}$ respectively, which are above the detection thresholds reported in (Benson et al. 1986). Participants completed a total of 8 blocks. Each block lasted 5 min and consisted of 50 heading trials, 40 standard ($p = 0.8$) and 10 target ($p = 0.2$) stimuli. For each block, left and right were assigned as targets so that each subject received 4 trials of left-target and 4 trials of right-target. This yielded a total of 320 standards and 80 targets per participant. The start of each trial was indicated by an auditory 10 ms beep, followed by the onset of motion after 1.5–2 s (uniform distribution). Following each motion, the platform returned to the start position via a subthreshold motion lasting approximately 5 s, thus ensuring that the participant had no indirect feedback about the previous motion. The standard and target were presented in a pseudo-random fashion, ensuring that at least three standard stimuli were presented between target stimuli. All participants were given two breaks lasting 5–10 min after the second and fifth block.

Participants were seated upon the motion platform while EEG data were acquired. Participants were instructed to fixate during stimulus delivery. Verbal instructions were given before each block as to which directions were the target and standard direction. Participants only responded to targets and the response-hand was counterbalanced across blocks. The standard and target stimulus were linear forward motions with a leftward or rightward heading of ±45° (Fig. 1c), which were counterbalanced, such that each participant completed four leftward and four rightward target blocks, consisting of two blocks in which they responded with their left-hand and two blocks with their right-hand. The standard and target were chosen such that they were perpendicular from each other and were well above the threshold of detection of non-visual heading reported in the literature (Telford et al. 1995; Fetsch et al. 2009; Butler et al. 2010, 2011; de Winkel et al. 2010).

Data processing

The EEG data were processed using the FASTER method (Nolan et al. 2010). This is an automated method of processing EEG data including filtering (1–95 Hz, with a notch filter at 50 Hz), averaging (1,500 ms epochs, 500 ms baseline and 1,000 ms after stimulus onset, grouped into correctly identified standard and target groups) and artifact removal (noisy epochs, channels, and independent components were removed). This method applies independent component analysis to subtract artifactual components, particularly EOG contributions, without removing EEG activity. This toolbox uses the data framework of the EEGLAB platform (Delorme and Makeig 2004).

Visualization using a 0.1 Hz filter revealed that some subjects' ERPs were dominated by very high-amplitude low-frequency content; therefore, we decided to use a 1 Hz filter that remedied this. During recording for one subject, the button response system malfunctioned. For this subject, we used all target epochs rather than only those with a correct response, as the overall false response rates were very low. They were also not included in the calculation of the response rates in Table 1.

Fig. 1 (*Left*) The outside of the Stewart platform. (*Middle*) During this study, a cloth sheet covered the platform to mask visual motion cues, and a Biosemi Active Two EEG system was installed to record EEG data. (*Right*) Top-down view of the experiment. Example of the vestibular heading oddball task, using a motion platform, participants were translated forward along two possible linear heading directions $\theta = \pm 45°$, *left* and *right*, which were alternatively the standard ($p = 0.8$) and target ($p = 0.2$) stimuli

Table 1 The group average and standard deviation of the reaction times, and true-/false-positive rates for the target

Measure	Value (mean ± SD)	Intraparticipant SD (ms)
Reaction time, overall (ms)	876 ± 214	57 ± 24
Reaction time, right (ms)	872 ± 223	67 ± 34
Reaction time, left (ms)	886 ± 221	61 ± 51
Hit rate, right (%)	95.14 ± 5.60	–
Hit rate, left (%)	93.91 ± 9.36	–
False-positive, right (%)	0.44 ± 1.12	–
False-positive, left (%)	0.7 ± 1.90	–

EEG analysis

Epoched data were separated into two groups, standard stimulus and target stimulus, to detect the P3 waveform. These groups were further separated into left- and right-going motions, in order to test for the effect of directionality. Event-related potentials (ERPs) were computed for each group. To test for the presence of the P3, mean amplitude measurements were obtained in a 100 ms window centered at the group-mean peak latency for the largest component. From the literature, frontal (Fz), central (Cz), and parietal (Pz) midline electrodes were identified as regions of interest for initial investigation.

Next, we take advantage of the full 128-channel high-density recording to identify with good spatial accuracy the spatio-temporal extent of the P3 distribution on the scalp, to perform source localization on the P3 waveform, and to demonstrate the P3 feature's validity on the single-participant level.

To achieve this, statistic parametric maps were first created across the entire scalp and across time in order to test for topographical differences in ERP amplitude between the standard and target conditions (Garrido et al. 2008), and also between leftward and rightward target conditions, and left- and right-hand button-press conditions. SPM 8 software was employed for analysis (http://www.fil.ion.ucl.ac.uk/spm). Data from each participant were transformed into two-dimensional scalp-space (interpolated from 128 channels) over each time sample during post-stimulus times from 0 to 1,000 ms for each condition separately. This transformation produced a three-dimensional spatiotemporal characterization of the ERP, which was then compared between conditions. A temporal epoch of interest of 300–950 ms was applied for the SPM analysis of the P3. The significance level was set at $p < 0.05$ and a stringent family-wise error (FWE) threshold was implemented, producing images that display only areas which are significantly different between the standard and target conditions following correction for multiple comparisons. The FWE correction implements aspects of random Gaussian field theory to deal with Type I errors due to the multiple comparisons inherent in EEG (Friston 1995). The Euler characteristic is computed to estimate the number of spatially independent elements in each scalp-slice and hence calculate the appropriate error rate base on this. It is necessary to apply smoothing to the image prior to computation of the family-wise error rate, using a Gaussian smoothing kernel. That used here was 6 × 6 × 8 voxels FWHM.

Statistical analysis was also performed on ERPs at a single-participant level. A bootstrapped t test ($N_{boot} = 2{,}000$ t tests) between standard and target epochs was applied to a 100 ms average at a 5-electrode average centered on the parietal central site (Pz) around the individual average peak values, selected as the maximum value in the individual participant's average target ERP from 300 to 950 ms. For one subject (S11 in Fig. 6), the detected peak was not the P3 peak and this was corrected manually. For each t test, a subset of target and standard epochs were randomly selected from all of the participant's available target and standard epochs, respectively. The number of standard target epochs selected in the bootstrapping process was increased in steps of 10 targets and 40 standards to correspond with the 20–80 % target-standard probabilities (Manly, 2006). The bootstrapping process continued until ≥95 % of t tests between the standard and target epochs were significant ($p < 0.05$). This ensured statistical significance on an individual level and also enabled the computation of the minimum number of epochs necessary for the detection of a difference between the target and standard epochs.

Further analyses of the P3 waveform in the frequency domain and using source analysis are detailed in the supplemental material.

Results

Behavioral results

Mean and standard deviations of reaction times and hit rates in response to targets were computed for each motion direction, see Table 1.

To ensure that there was no difference between target directions, the left- and right-target reaction times, true-positives and false-positives were submitted to paired t tests. The tests revealed no significant difference, $t_{13} = -1.836$, $p = 0.0893$, $t_{13} = -0.3340$, $p = 0.744$, and $t_{13} = -0.582$, $p = 0.572$, respectively. These tests were performed on 14 of 15 subjects, as for one subject, the response button malfunctioned.

EEG results

Figure 2 depicts the ERPs for standard (black) and target (gray) conditions along the midline electrodes. The waveforms are seen to be maximally different at 600 ms, with highest target amplitude at Pz—this is the P3 peak. A 100 ms window (±50 ms) around this peak was chosen for preliminary analysis on these electrodes and is denoted by the highlighted section in Fig. 2.

Figure 3 displays topographical plots of the group average standard (A) and target (B). From these topographies, we can see the target ERP's divergence at 400 ms from the standard ERP, and the parieto-central peak, which starts at 500 ms, is maximum at 600 ms and wanes at 700 ms.

Preliminary statistical analysis was performed on this peak (100 ms average from 550 ms to 650 ms) along the midline electrodes Fz, Cz and Pz. A 2-way ANOVA showed main effects of both Standard vs. Target ($F_{1,86} = 7.2$, $p = 0.0087$) and electrode ($F_{2,86} = 39.67$, $p < 0.0001$). Figure 4 depicts the means, with standard error bars, of the 600 ms peak at these midline electrodes.

To gain a deeper understanding of the spatiotemporal properties of the P3 waveform we conducted further analysis using a paired t test design in SPM. Figure 5 shows the results of the spatio-temporal SPM analysis. This plot displays the areas of significant difference in the ERP, on the scalp and across time. The non-white areas shown in Fig. 5 are those with significant difference between target and standard conditions (target > standard) after FWE correction at $p < 0.05$. Significant cutoff after FWE correction was $t_{14} \geq 6.68$.

Further SPM analyses showed no significant difference between left- and right-going target ERPs ($p > 0.05$), or between left- and right-handed button-press target ERPs ($p > 0.05$).

The differences in the P3 peak can be seen to be present at the single-participant level, as illustrated in Fig. 6 for all participants. Individual participant bootstrap analysis revealed that 14 of 15 participants exhibited significantly different values between standard and target ERPs at the individual P3 peak. Furthermore, the critical number of target epochs necessary to detect this difference was found

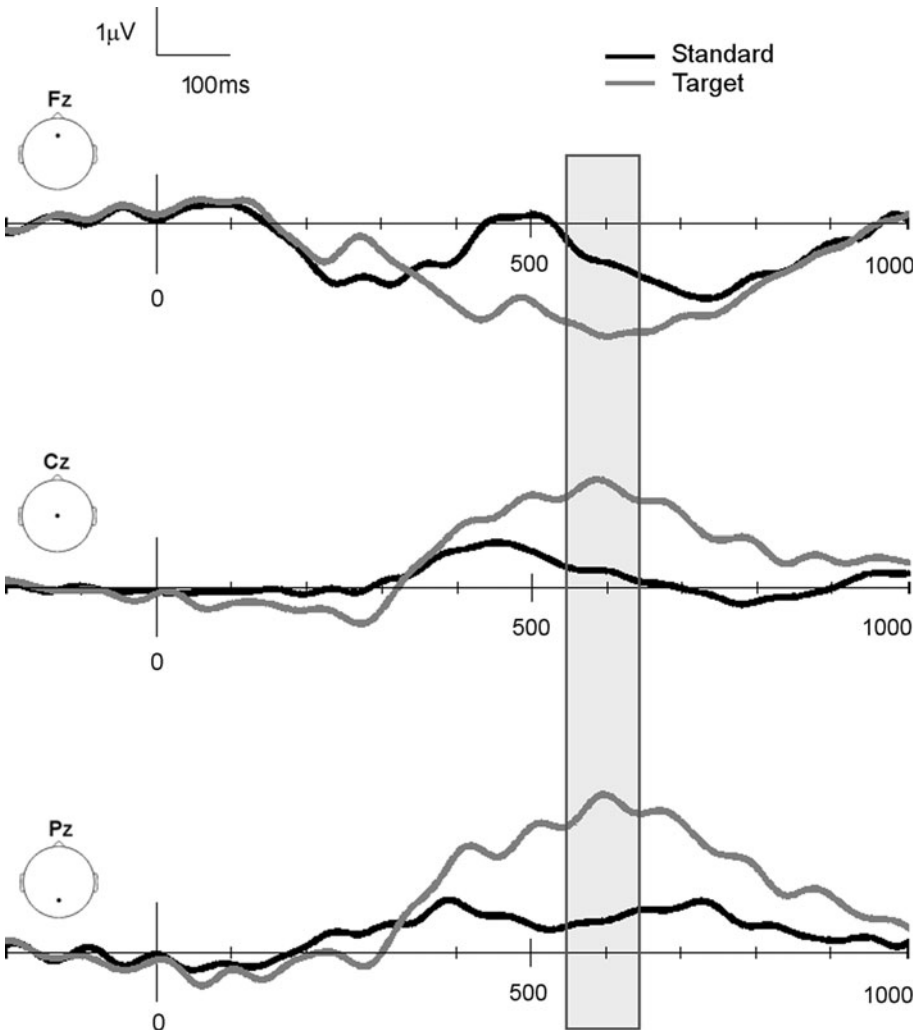

Fig. 2 Group average standard (*black*) and target (*gray*) ERPs calculated from Fz (**a**), Cz (**b**) and Pz (**c**), after epoching relative to the motion onset. The highlighted section indicates the temporal region of interest for peak analysis

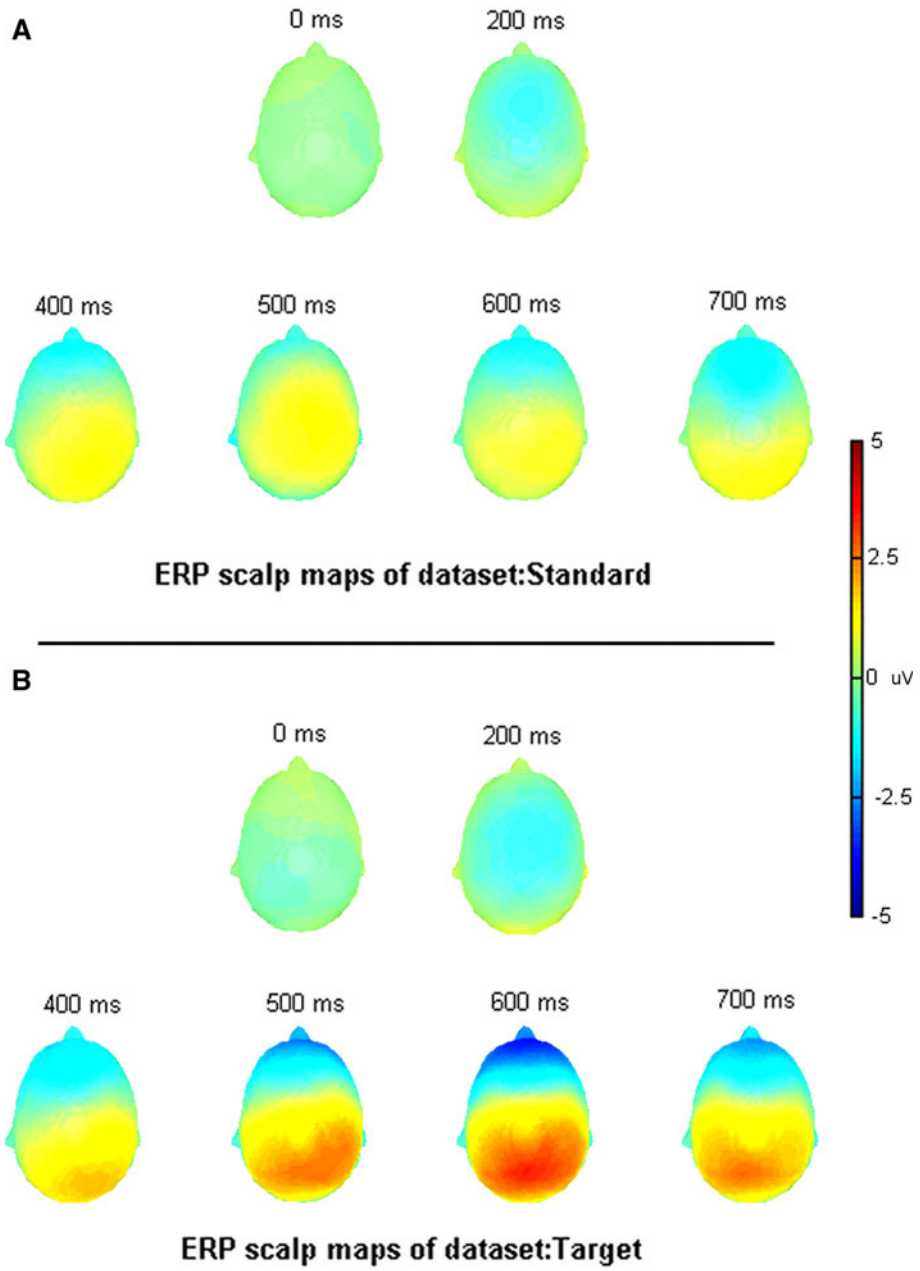

Fig. 3 Topographic representations of **a** the standard ERP and **b** the target ERP

to be within the 95 % confidence interval of 43.78–70.07 epochs. A conservative estimate of 80 targets, which we used here, would be suitable. Thus, the vestibular P3 is seen to be a measure that can be applied on a single-participant basis, and we have found the approximate minimum number of trials necessary for implementation on a single-participant level.

Discussion

In this study, we investigated the electrophysiological correlates of the detection of a vestibular heading oddball stimulus in which participants were translated ~8 cm along a standard or target one second linear heading direction. The results reveal a waveform with a parieto-central distribution (see Fig. 5) which is a typical P3 topography (see Polich and Heine 1996), indicating that vestibular oddball stimuli are processed in a similar fashion as other sensory modalities.

Human behavioral experiments have shown that the vestibular system is used in a wide range of tasks, for example, cortical control of visual saccades (Israel et al. 1995), spatial updating (Campos et al. 2009), and heading perception (Fetsch et al. 2009; Butler et al. 2010). Furthermore, recent progress in simulator design (Groen and

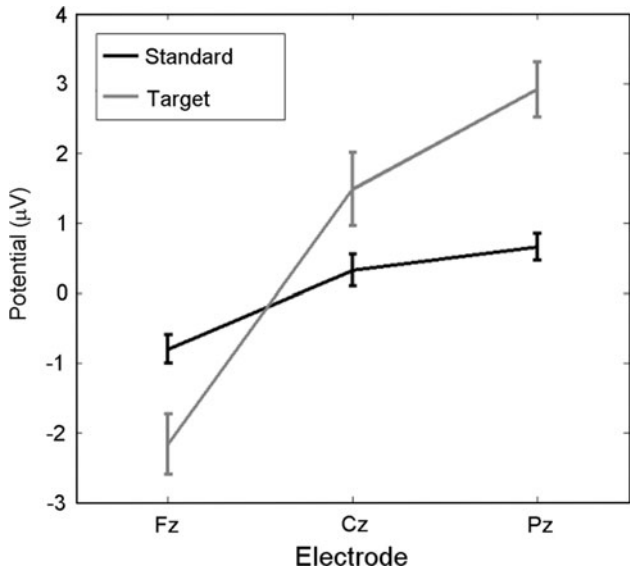

Fig. 4 Mean amplitudes of the P3 peak at midline electrodes; *error bars* represent standard error of the mean

Bles 2004; Teufel et al. 2007) have made it feasible to reproduce large ranges of motion to gain further understanding of complex control tasks, such as "pilot in the loop" behavior (Nieuwenhuizen et al. 2009). While all these advances have furthered the understanding of the role non-visual cues in self-motion perception, there is little research into the cortical representation of vestibular processing in humans. The vestibular P3 presents an elegant approach to understanding the neural correlates of non-visual self-motion change detection processing.

The typical nature of the vestibular P3 lends weight to the argument that vestibular signals are treated and processed in the brain in a similar fashion to other sensory signals, as the P3 is known to be representative of cognitive processes (Polich 1993) and hence reflects the cognitive processing of sensory information. The 2-stimulus oddball paradigm used here evokes a P3b response, which is associated with updating of the internal representation of the environmental context (Polich 2007). The P3b is known to have a parieto-central topographic distribution, consistent with the results seen here. While the typical nature of the P3 might seem like an intuitive result, it is not entirely obvious. There is still an ongoing debate within the self-motion behavioral literature about the utility of vestibular signals in human self-motion perception. A number of studies have shown that the introduction of non-visual self-motion cues signals are not beneficial to self-motion perception (Telford et al. 1995; Ohmi 1996; de Winkel et al. 2010; Butler et al. 2011), and hence the vestibular cues might not be processed in a similar fashion to other sensory modalities. On the other hand, recent studies have shown an optimal benefit to the introduction of vestibular signals in the discrimination of heading (Fetsch et al. 2009; Butler et al. 2010, 2011), which is more in line with the typical nature of the vestibular P3 presented here.

The long latency of the P3 and response can be contrasted with the reflexive responses initiated by the vestibular system. The vestibulo-collic reflex has a latency in the order of tens of milliseconds in response to a step stimulus (Séverac Cauquil et al. 2003). However, as the P3 latency is at approximately 600 ms, and the response

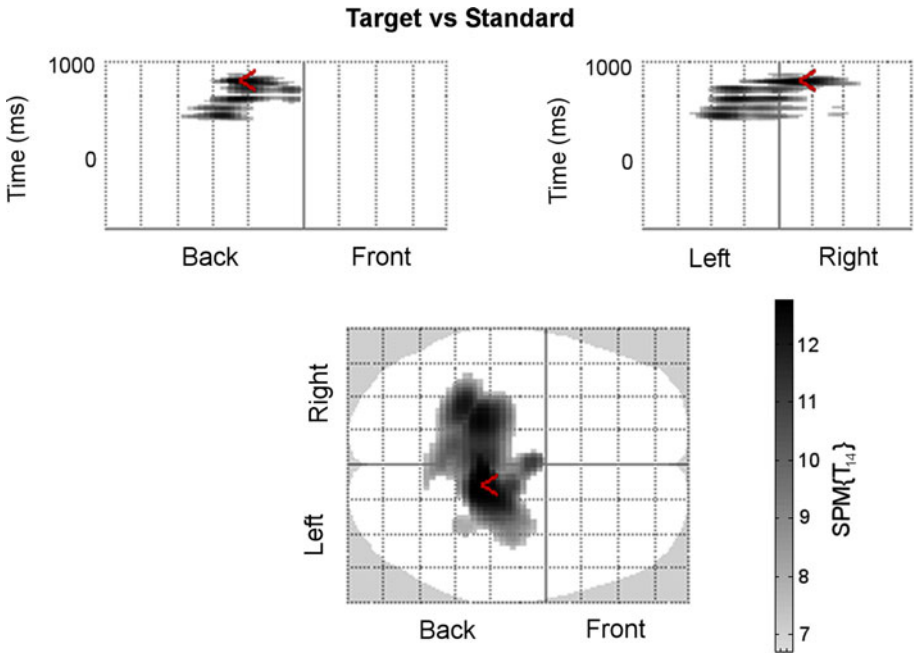

Fig. 5 SPM output showing temporal and topographical differences between the standard and target conditions

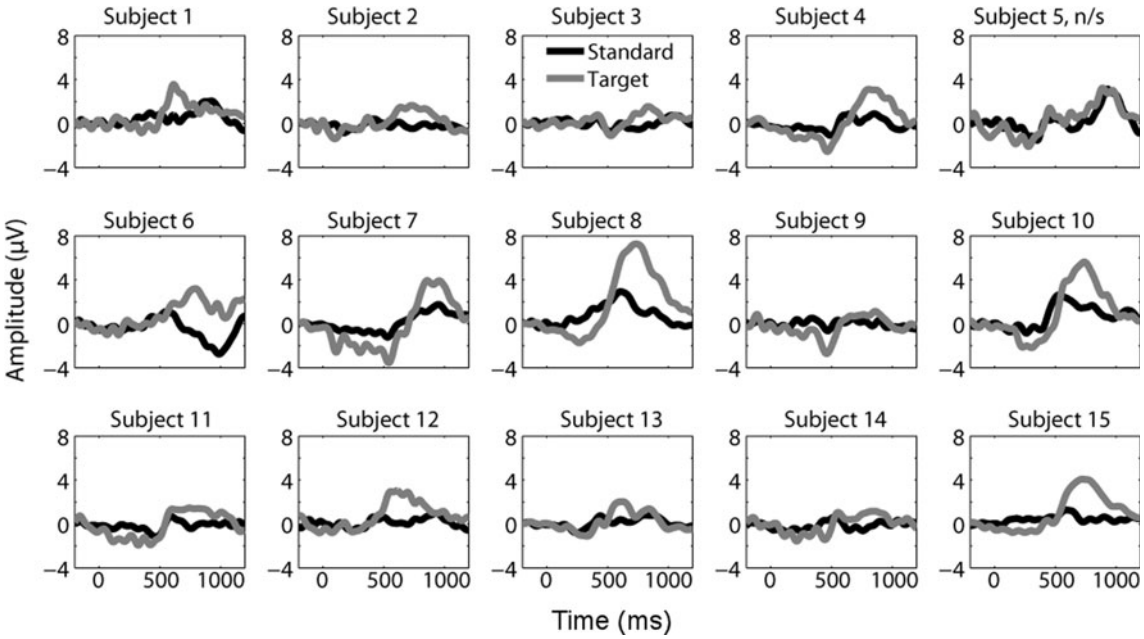

Fig. 6 Individual participants' average standard (*black*) and target (*gray*) ERPs at the 5-channel average around the parietal central site (Pz). All subjects exhibit significant difference between standard and target at their individual target peaks except for the one subject marked "n/s". 20 Hz low-pass filter applied for display only

latency is 876 ms, we can see that cognitive processing of motion stimuli is slow, especially compared with the autonomic responses that are resultant of motion. This has been noted previously (Baxter and Travis 1938), and it has also been seen behaviorally that responses to rotational (Barnett-Cowan and Harris 2009) and translational (Barnett-Cowan et al. 2010) vestibular motion stimuli are slower than responses to visual and auditory stimuli. Another consideration is that the sinusoidal acceleration motion stimulus used here is quite different from the discrete stimuli used in auditory and visual experiments, and therefore, the discrimination between the target and standard is not instantaneous and so some delay is expected. Future experiments are required to investigate the nature of this delay as it could give insight into the time course of the perception of vestibular cues.

The use of non-visual self-motion stimuli to evoke vestibular responses has been used in animal studies (Bremmer et al. 2002a, b; Gu et al. 2007, 2008, 2010). In these studies, it is common to regard somatosensory influence as minimal and label such stimuli as vestibular stimuli. To understand the vestibular and somatosensory contributions to linear non-visual self-motion perception, Walsh (1961) minimized the somatosensory inputs and found that these only made a small difference in motion detection thresholds. Furthermore, Gu et al. (2007) showed that the detection threshold for non-visual heading stimuli was increased 50 times after vestibular lesioning in macaque monkeys. In accordance with these studies and the data from this study, we consider the P3 response recorded here to be primarily driven by the detection of an oddball vestibular stimulus and thus its implications can be considered in the context of vestibular processing.

As this study deals with movement and EEG data, the issue of interference from EMG to EOG signals was important to consider due to the vestibulo-collic and vestibulo-ocular reflexes. EMG contamination is seen to be a broadband phenomenon and can peak in the beta band, as seen in the contamination study by (Goncharova 2003). They do, however, also show increases in gamma band activity in both muscle groups studied. Time–frequency analysis of the ERP data revealed that there were significant differences in the beta band, but very little significant low or high gamma (30–100 Hz) activity (for more details see Supplementary Materials). Furthermore, the parieto-central topographic peak of the ERPs does not exhibit the strong activity at the edges of the scalp that are typical of EMG activity. From this analysis, we conclude that there is minimal contribution from EMG to the recorded response. With regard to EOG activity, the parieto-central topographic distribution again is not in concordance with the unipolar frontal topographies obtained from EOG activity. We have also shown with preliminary results that the generators of vestibular ERPs in the same experimental arrangement, using a similar paradigm, are sensible in light of the literature (Nolan et al. 2011b). The concordance of the sLORETA results presented in the supplemental material with literature also supports these claims.

The visual, auditory and olfactory P3 have been used to shed light on functional differences between controls and patients with a variety of diseases (Polich 1998), including Multiple Sclerosis (MS) (Whelan et al. 2010) and Alzheimer's disease (Juckel et al. 2008; Morgan and Murphy 2002). Features of the visual P3 component have been shown to be a reliable biomarker; for example, Whelan et al. (2010) show that P3 peak amplitude and latency abnormalities have a high correlation with cognitive impairment in patients with MS.

It has been seen recently (Setti et al. 2011) that audio-visual multisensory integration is less efficient in older subject who fall compared with older non-fallers. The perception of temporally distinct stimuli as concurrent was seen to happen for considerably longer temporal intervals, manifesting as the incorrect multisensory integration of stimuli separated by 270 ms. At this extended time scale, this could indicate a top-down problem in modulating the cognitive processing of sensory information, rather than a problem of sensory decline, and so the phenomenon may not be specific to audio-visual sensory modalities. It has been seen that while complaints of stability are common, caloric vestibular tests (which measure semicircular canal function) do not degrade with age (Mallinson 2004). This may imply that compromised processing of vestibular information, rather than purely sensory organ degradation, play a part in elder instability. Thus, the relationship between instability and vestibular function is not straightforward, and further research is necessary. As the P3 is also a measurement of the processing of sensory information, it has the potential to be to be investigated as a biomarker.

To this end, we have shown, using a bootstrapping procedure, that 86.7 % of participants exhibit a clear P3 component; furthermore, we identified a conservative minimum number of target trials required for individual statistical analysis of the P3. This enables the possibility of using the motion-based P3 for testing of vestibular stimulus processing in individual participants. It should be noted that we used a 1 Hz high-pass filter which has been shown to reduce P3 amplitude (Kappenman 2010), however, initial visualization of the ERPs with a high-pass filter at 0.1 Hz revealed a slow wave component which dominated a number of subjects' ERPs and appeared primarily to be an artifact of the full body motion stimuli due to its large amplitude. Furthermore, it has been shown that using button responses also reduces the amplitude of the P3 (Salisbury 2003); for the purposes of this study, button response was practical and allowed us to measure reaction times and correct identification, and the P3 response was robust enough to be detected even at the single subject-level regardless of these attenuations. It may, however, be possible to reduce trial number requirements by addressing some of these factors.

The use of a Stewart platform and a high-density electrode grid were important to establish the vestibular P3 using precise and controlled stimuli and to confirm that the topographical distribution was similar to that of other modalities. This validation enables the use of an inexpensive arrangement with, for example, three electrodes and a unidirectional motion track. Such practical arrangements have greater clinical application. Future experiments could also extend the scope of this cognitive motion processing paradigm by investigating whether a 3-stimulus paradigm evokes a topographically distinguishable P3a waveform, as is seen in literature (Polich 2007).

In summary, this study has demonstrated that a motion oddball stimulus evokes a vestibular-based P3 ERPs, which is similar in its morphology to the P3 in other modalities. The validation of this methodology provides a strong grounding on which to investigate the processes of vestibular cues and could be a useful tool in understanding vestibular disorders.

Acknowledgments Funding: This study was partly funded by an Irish Research Council for Science Engineering and Technology Postgraduate scholarship to H. Nolan, a Science Foundation Ireland grant to R. Reilly 09/RFP/NE2382, a WCU (World Class University) program funded by the Ministry of Education, Science and Technology through the National Research Foundation of Korea (R31-10008) to H. Bülthoff. Dr. Foxe is supported by a grant from the U.S. National Institute of Mental Health (NIMH R01 MH85322). The authors would like to thank Kevin Whittingstall for invaluable advice and guidance. We would like to thank Julian Hofmann, Frank Nieuwenhuizen and Michael Weyel for help with the experimental arrangement. Preliminary results from this work were presented at IEEE EMBC Conference, Boston, 2011.

References

Angelaki DE, Cullen KE (2008) Vestibular system: the many facets of a multimodal sense. Annu Rev Neurosci 31:125–150

Barnett-Cowan M, Harris L (2009) Perceived timing of vestibular stimulation relative to touch, light and sound. Exp Brain Res 198:221–231

Barnett-Cowan M, Nolan H, Butler JS, Foxe JJ, Reilly RB, Bülthoff HH (2010) Reaction time and event-related potentials to visual, auditory and vestibular stimuli. J Vis 10:1400

Baxter B, Travis RC (1938) The reaction time to vestibular stimuli. J Exp Psychol 22:277–282

Benson AJ, Spencer MB, Stott JR (1986) Thresholds for the detection of the direction of whole-body, linear movement in the horizontal plane. Aviat Space Environ Med 57:1088–1096

Bremmer F, Duhamel JR, Ben Hamed S, Graf W (2002a) Heading encoding in the macaque ventral intraparietal area (VIP). Eur J Neurosci 16:1554–1568

Bremmer F, Klam F, Duhamel JR, Ben Hamed S, Graf W (2002b) Visual-vestibular interactive responses in the macaque ventral intraparietal area (VIP). Eur J Neurosci 16:1569–1586

Butler JS, Smith ST, Campos JL, Bülthoff HH (2010) Bayesian integration of visual and vestibular signals for heading. J Vision 10:1–13

Butler JS, Campos JL, Bülthoff HH, Smith S (2011) The role of stereo vision in visual-vestibular integration. Seeing Perceiving 24(5): 453–470

Campos JL, Siegle JH, Mohler BJ, Bülthoff HH, Loomis JM (2009) Imagined self-motion differs from perceived self-motion: evidence from a novel continuous pointing method. PLoS ONE 4:e7793

de Winkel KN, Weesie J, Werkhoven PJ, Groen EL (2010) Integration of visual and inertial cues in perceived heading of self-motion. J Vision 10:1–10

Delorme A, Makeig S (2004) EEGLAB: an open source toolbox for analysis of single-trial EEG dynamics including independent component analysis. J Neurosci Methods 134:9–21

Fetsch CR, Turner AH, DeAngelis GC, Angelaki DE (2009) Dynamic reweighting of visual and vestibular cues during self-motion perception. J Neurosci 29:15601–15612

Fetsch CR, Rajguru SM, Karunaratne A, Gu Y, Angelaki DE, Deangelis GC (2010) Spatiotemporal properties of vestibular responses in area MSTd. J Neurophysiol 104:1506–1522

Friedman D, Cycowicz YM, Gaeta H (2001) The novelty P3: an event-related brain potential (ERP) sign of the brain's evaluation of novelty. Neurosci Biobehav Rev 25:355–373

Friston KJ, Holmes AP, Worsley KJ, Poline JB, Frith CD, Frackowiak RSJ (1995) Statistical parametric maps in functional imaging: a general linear approach. Hum Brain Mapp 2:189–210

Garrido MI, Friston KJ, Kiebel SJ, Stephan KE, Baldeweg T, Kilner JM (2008) The functional anatomy of the MMN: a DCM study of the roving paradigm. Neuroimage 42:936–944

Goncharova II, McFarland DJ, Vaughan TM, Wolpaw JR (2003) EMG contamination of EEG: spectral and topographical characteristics. Clin Neurophysiol 114:1580–1593

Gramann K, Gwin JT, Bigdely-Shamlo N, Ferris DP, Makeig S (2010) Visual evoked responses during standing and walking. Front Hum Neurosci 4:202

Groen EL, Bles W (2004) How to use body tilt for the simulation of linear self motion. J Vestibul Res-Equil 14:375–385

Gu Y, DeAngelis GC, Angelaki DE (2007) A functional link between area MSTd and heading perception based on vestibular signals. Nat Neurosci 10:1038–1047

Gu Y, Angelaki DE, DeAngelis GC (2008) Neural correlates of multisensory cue integration in macaque MSTd. Nat Neurosci 11:1201–1210

Gu Y, Fetsch CR, Adeyemo B, Deangelis GC, Angelaki DE (2010) Decoding of MSTd population activity accounts for variations in the precision of heading perception. Neuron 66:596–609

Gwin JT, Gramann K, Makeig S, Ferris DP (2010) Removal of movement artifact from high-density EEG recorded during walking and running. J Neurophysiol 103:3526–3534

Hofferberth B (1995) The clinical significance of vestibular evoked potentials (REP). Acta Otolaryngol 115:124–125

Hood JD, Kayan A (1985) Observations upon the evoked responses to natural vestibular stimulation. Electroenceph and Clin Neurophysiol 62:266–276

Israel I, Rivaud S, Gaymard B, Berthoz A, Pierrot-Deseilligny C (1995) Cortical control of vestibular-guided saccades in man. Brain 118:1169–1183

Juckel G, Clotz F, Frodl T, Kawohl W, Hampel H, Pogarell O et al (2008) Diagnostic usefulness of cognitive auditory event-related P300 subcomponents in patients with Alzheimers disease? J Clin Neurophys 25:147–152

Kappenman ES, Luck SJ (2010) The effects of electrode impedance on data quality and statistical significance in ERP recordings. Psychophysiology 47:888–904

Katayama JI, Polich J (1999) Auditory and visual P300 topography from a 3 stimulus paradigm. Clin Neurophysiol 110:463–468

Kolchev C (1995) Vestibular late evoked potentials (VbEP) processed by means of brain electrical activity mapping (BEAM). Acta Otolaryngol 115:130–133

Loose R, Probst T, Tucha O, Bablok E, Aschenbrenner S, Lange KW (2002) Vestibular evoked potentials from the vertical semicircular canals in humans evoked by roll-axis rotation in microgravity and under 1-G. Behav Brain Res 134:131–137

Lopez C, Blanke O (2011) The thalamocortical vestibular system in animals and humans. Brain Res Rev 67:119–146

MacNeilage PR, Banks MS, DeAngelis GC, Angelaki DE (2010) Vestibular heading discrimination and sensitivity to linear acceleration in head and world coordinates. J Neurosci 30:9084–9094

Mallinson AI, Longride NS (2004) Caloric response does not decline with age. J Vestib Res 14:393–396

Manly BFJ (2006) Boostrap tests. In: Manly BFJ (ed) Randomization, bootstrap and Monte Carlo methods in biology, 3rd edn. Chapman & Hall, Boca Raton, pp 99–101

Morgan CD, Murphy C (2002) Olfactory event-related potentials in Alzheimer's disease. J Internat Neuropsych Soc 8:753–763

Morgan CD, Geisler MW, Covington JW, Polich J, Murphy C (1999) Olfactory P3 in young and older adults. Psychophysiol 36:281–287

Nieuwenhuizen FM, Zaal PMT, Mulder M, van Paassen MM, Mulder JA (2009) Modeling human multi-channel perception and control using linear time-invariant models. J Guid Control Dyn 31:999–1013

Nolan H, Whelan R, Reilly RB, Bulthoff HH, Butler JS (2009) Acquisition of human EEG data during linear self-motion on a Stewart platform. 4th International IEEE/EMBS Conference on Neural Engineering. Antalya, Turkey, pp 585–588

Nolan H, Whelan R, Reilly RB (2010) FASTER: fully automated statistical thresholding for EEG artifact rejection. J Neurosci Methods 192:152–162

Nolan H, Butler JS, Whelan R, Foxe JJ, Bulthoff HH, Reilly RB (2011a) Motion P3 demonstrates neural nature of motion ERPs. 33rd annual international conference of the IEEE engineering in medicine and biology society. Boston, USA, pp 3884–3887

Nolan H, Butler JS, Whelan R, Foxe JJ, Bulthoff HH, Reilly RB (2011b) Electrophysiological source analysis of passive self-motion. Neural Engineering (NER), 2011 5th International IEEE/EMBS Conference on, pp 53–56

Ohmi M (1996) Egocentric perception through interaction among many sensory systems. Brain Res Cogn Brain Res 5:87–96

Polich J (1993) Cognitive Brain Potentials. Curr Directions in Psych Sci 2:175–179

Polich J (1998) P300 clinical utility and control of variability. J Clin Neurophysiol 15:14–33

Polich J (2007) Updating P300: an integrative theory of P3a and P3b. Clin Neurophysiol 118:2128–2148

Polich J, Heine MR (1996) P300 topography and modality effects from a single-stimulus paradigm. Psychophysiology 33:747–752

Rodionov V, Elidan J, Sohmer H (1996) Analysis of the middle latency evoked potentials to angular acceleration impulses in man. Electroenceph and Clin Neurophysiol 100:354–361

Salisbury DF, Rutherford B, Shenton ME, McCarley RW (2003) Button-pressing affects P300 amplitude and scalp topography. Clin Neurophysiol 112:1676–1684

Setti A, Burke KE, Kenny RA, Newell F (2011) Is inefficient multisensory processing associated with falls in older people? Exp Brain Res 209:375–384

Séverac Cauquil A, Faldon M, Popov K, Day BL, Bronstein AM (2003) Short-latency eye movements evoked by near-threshold galvanic vestibular stimulation. Exp Brain Res 148:414–418

Sutton S, Braren M, Zubin J, John ER (1965) Evoked-potential correlates of stimulus uncertainty. Science 150(700):1187–1188

Telford L, Howard IP, Ohmi M (1995) Heading judgments during active and passive self-motion. Exp Brain Res 104:502–510

Teufel HJ, Nusseck H-G, Beykirch KA, Butler JS, Kerger M and Bülthoff HH (2007) MPI Motion Simulator: Development and Analysis of a Novel Motion Simulator. AIAA Modeling and Simulation Technologies Conference and Exhibit

von der Heyde M (2001) A distributed virtual reality system for spatial updating: concepts, implementation, and experiments. Dissertation, Universität Bielefeld

Walsh EG (1961) Role of the vestibular apparatus in the perception of motion on a parallel swing. J Physiol 155:506–513

Whelan R, Lonergan R, Kiiski H, Nolan H, Kinsella K, Bramham J et al (2010) A high-density ERP study reveals latency, amplitude, and topographical differences in multiple sclerosis patients versus controls. Clin Neurophysiol 121:1420–1426